

PROF. G. KONECNY*
Univ. of New Brunswick
Fredericton, N. B., Canada

Interior Orientation and Convergent Photography

ABSTRACT: Convergent photography, though awkward in use, yields a significant theoretical accuracy increase over vertical photography. The practical accuracy is lower than theoretically expected, mainly due to errors of interior orientation. These affect the accuracy of relative orientation for convergent photographs. More responsive procedures are suggested for orientation and bridging. Practical test results indicate that accuracy can thus be considerably improved.

INTRODUCTION

The idea of convergent photography is as old as stereo-photogrammetry. Convergent photographs were used from balloons around 1900, (S. Finsterwalder, 1903, pp. 225-260), a long time before the airplane would permit a mechanized sequence of vertical photographs.

In 1926, a convergent photography procedure by twin cameras was developed to increase the intersection accuracy of corresponding photogrammetric rays. By the introduction of wide-angle photography in 1934, however, an increase of accuracy could also be achieved, without having to give up the simplicity of viewing and measuring from vertical photographs.

Despite the difficulties in stereovision, due to wide variations of scale and despite the complexity of the system, wide-angle convergent photography was reintroduced in the 1950's by the U. S. Geological Survey to further economize plotting and bridging. Super-wide angle development again stopped the widespread use of convergent photography.

Today not primarily economic considerations but increased accuracy still open perspectives for convergent photography.

It has been shown that for special projects such as flood control surveys and for certain engineering projects, extreme accuracies, unachieved by vertical photography, could be attained, particularly from low altitudes.

The peculiarities and the awkwardness of working with convergent photography naturally have led only to limited acceptance of convergent procedures. On the other hand, though, theoretical considerations have always shown (Hallert, 1954) that convergent photography should yield a sizeable increase in accuracy, this has not been found in practice as Table 1 shows.



PROF. G. KONECNY

* Paper presented at the Semiannual Meeting of the American Society of Photogrammetry, 1963.

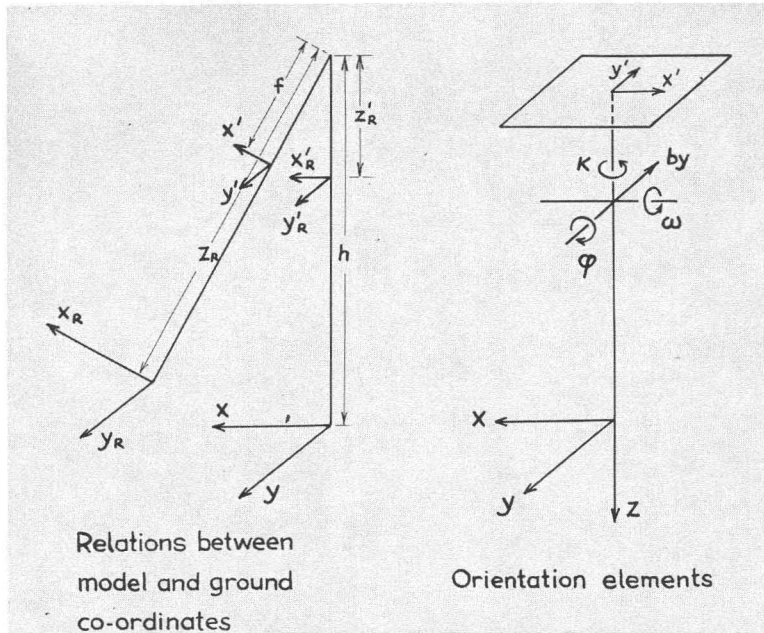


FIG. 1. Relations between Model and Ground Coordinates and Orientation Elements.

Tests conducted by AMS (Theis 1958) and by ERDL (Pennington 1954) show for the most part only an insignificant accuracy increase for convergent photography, or a decrease of accuracy for convergent bridging procedures.

TABLE 1
PRACTICAL ACCURACY REACHED WITH CONVERGENT PHOTOGRAPHY

Author	Year	Instrument	Procedure	m_p m_h in $\%$ of h	
				± 1.67 $\%$ of h	± 0.71 $\%$ of h
Pennington ERDL	1954	Multiplex	Bridging 6 models		
Theis AMS	1958	Kelsh	WA ¹ vert. points		± 0.17
			WA conv. points		± 0.16
		Balplex	WA vert. points		± 0.24
			WA conv. points		± 0.21
		Kelsh	WA vert. contours		± 0.24
			WA conv. contours		± 0.18
Balplex	1958	C8	WA vert. bridging 15 models		± 0.18
			WA conv. bridging 8 models		± 0.33
Griffin ERDL	1959	C8 and BL 720	WA vert. bridging 16 models	± 1.55	± 0.69
		C8 and BL 720	WA conv. bridging 8 models	± 1.59	± 0.54

¹ WA = wide-angle.

More recent investigations have led to the cause of this (E. P. Griffin, 1959) (G. Konecny, 1962), but the right conclusions have generally not yet been drawn. Particularly the errors in interior orientation have led to difficulties in attaining the expected theoretical accuracy.

INTERIOR ORIENTATION ERRORS AND MODEL DEFORMATIONS

If x, y, h designate ground co-ordinates, x', y', f photo co-ordinates, $x_R, y_R, f_R, x_R', y_R', z_R'$ rotated ground and photo co-ordinates, and A an orthogonal rotational matrix, we have the well-known perspective relations:

$$\begin{pmatrix} x \\ y \\ h \end{pmatrix} = A \begin{pmatrix} x_R \\ y_R \\ z_R \end{pmatrix}; \quad \begin{pmatrix} x_R' \\ y_R' \\ z_R' \end{pmatrix} = A \begin{pmatrix} x' \\ y' \\ f \end{pmatrix};$$

$$x = \frac{h}{z_R} x_R; \quad y = \frac{h}{z_R} y_R; \quad x' = \frac{f}{z_R'} x_R'; \quad y' = \frac{f}{z_R'} y_R'$$

from which we obtain by linearization and differentiation the complete differential relations between model co-ordinates (x, y, h) and exterior ($d\phi, d\omega, d\kappa$) as well as interior orientation elements (dx', dy', df). (See Figure 1.)

For a rotational sequence ϕ, ω, κ and the signs of the CS we obtain:

$$\begin{aligned} dx &= h \left(1 + \frac{x^2}{h^2} \right) d\phi + \frac{y}{h} (h \sin \phi - x \cos \phi) d\omega - \frac{y}{h} (h \cos \phi + x \sin \phi) d\kappa \\ &\quad - \frac{x}{h} dbz + dbx + \frac{1}{hf} (h \cos \phi + x \sin \phi)^2 dx' \\ &\quad + \frac{1}{hf} (h \sin \phi - x \cos \phi) (h \cos \phi + x \sin \phi) df; \\ dy &= \frac{xy}{h} d\phi - \left[x \sin \phi + h \cos \phi \left(1 + \frac{y^2}{h^2} \right) \right] d\omega + \left[x \cos \phi - h \sin \phi \left(1 + \frac{y}{h^2} \right) \right] d\kappa \\ &\quad - \frac{y}{h} dbz - dby + \frac{1}{hf} [y \sin \phi (x \sin \phi + h \cos \phi)] dx' \\ &\quad + \frac{1}{f} (x \sin \phi + h \cos \phi) dy' - \frac{1}{hf} y \cos \phi (x \sin \phi + h \cos \phi) df \end{aligned}$$

for use with "base outside" we get:

$$py = dy_R - dy_L$$

$$px = dx_R - dx_L; \quad dh = \frac{h}{b} px,$$

characterizing model deformations. A graphical representation shows that elements $d\omega, d\kappa, dx', dy', df$ act differently in convergent and near vertical photographs, while $d\phi$ acts the same. (See Figure 2.)

As is well known, interior orientation errors are not harmful to vertical photography except for translations of the model in the x, y and z directions. For convergent photographs, however, an erroneous relative orientation will result, since the y parallaxes introduced by dx', dy' and df will cause an erroneous compensation of these parallaxes by other elements:

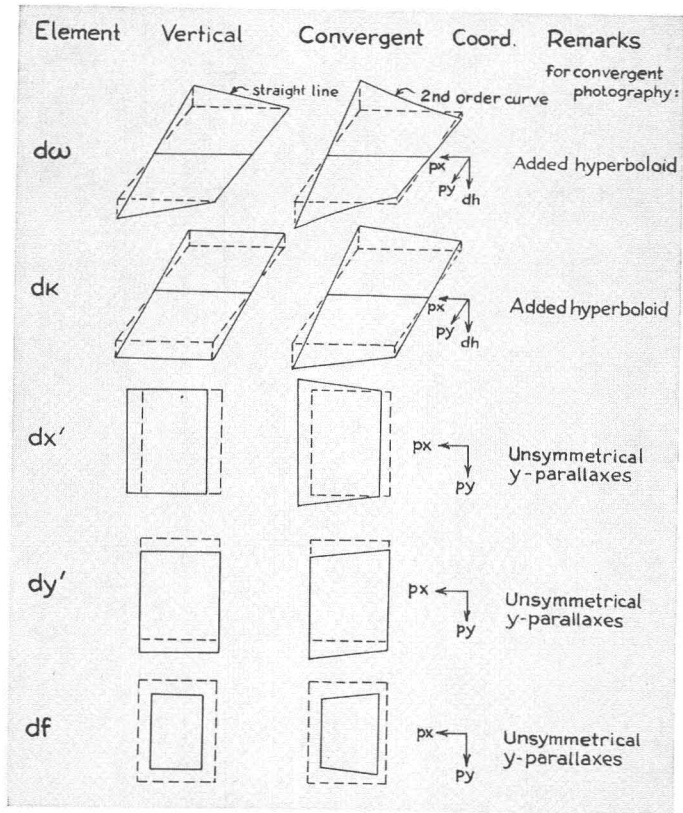


FIG. 2. Model Deformation for Vertical and Convergent Photography.

0.1 mm dx' will be compensated by $+0.15^c d\phi - 0.05$ mm dbz

0.1 mm dy' will be compensated by $-0.67^c dk - 0.17^c d\omega$

0.1 mm df will be compensated by $-0.69^c d\phi - 0.22$ mm dbz .

Analytically this can be expressed as follows: Using the model co-ordinates of the orientation points 1 to 6 in the formula

$$\begin{aligned}
 py &= \frac{1}{f_R h} (xy \sin^2 \phi + yh \sin \phi \cos \phi) dx_R' + \frac{1}{f_R h} (xh \sin \phi + h^2 \cos \phi) dy_R' \\
 &+ \frac{1}{f_R h} (-xy \sin \phi \cos \phi - yh \cos^2 \phi) df_R \\
 &+ \frac{1}{f_L h} (-(x-b)y \sin^2 \phi - yh \sin \phi \cos \phi) dx_L' \\
 &+ \frac{1}{f_L h} (-(x-b)h \sin \phi - h^2 \cos \phi) dy_L' \\
 &+ \frac{1}{f_L h} ((x-b)y \sin \phi \cos \phi + yh \cos^2 \phi) df_L
 \end{aligned}$$

we obtain six expressions for parallaxes p_1 to p_6 which can be used to obtain the exterior orientation elements in terms of interior orientation errors:

$$\begin{aligned}
 d\phi_R &= -\frac{h}{2bd} ((p_3 - p_5) - (p_4 - p_6)) \\
 &= \sin^2 \phi \left(\frac{dx_R'}{f_R} - \frac{dx_L'}{f_L} \right) - \sin \phi \cos \phi \left(\frac{df_R}{f_R} - \frac{df_L}{f_L} \right); \\
 dbz_R &= +\frac{h}{2d} (p_4 - p_6) = h \sin \phi \cos \phi \left(\frac{dx_R'}{f_R} \right) - (b \sin^2 \phi - h \sin \phi \cos \phi) \left(\frac{dx_L'}{f_L} \right) \\
 &\quad + h \cos^2 \phi \left(\frac{df_R}{f_R} \right) + (b \sin \phi \cos \phi - h \cos^2 \phi) \left(\frac{df_L}{f_L} \right); \\
 dby_R &= +\frac{h^2}{4d^2} [(p_3 + p_4 + p_5 + p_6 - 2p_1 - 2p_2)] + \frac{1}{6} [(p_1 - p_2) + (p_3 - p_4) + (p_5 - p_6)] \\
 &\quad - \frac{1}{2} [(p_1 + p_2)] = h \cos \phi \left(\frac{dy_R'}{f_R} - \frac{dy_L'}{f_L} \right); \\
 d\kappa_R &= -\frac{h}{4d^2} \sin \phi (p_3 + p_4 + p_5 + p_6 - 2p_1 - 2p_2) \\
 &\quad + \frac{1}{3b} \cos \phi (p_1 - p_2 + p_3 - p_4 + p_5 - p_6) \\
 &= \sin \phi \cos \phi \left(\frac{dy_R'}{f_R} - \frac{dy_L'}{f_L} \right) \\
 d\omega_R &= -\frac{h}{4d^2} \cos \phi (p_3 + p_4 + p_5 + p_6 - 2p_1 - 2p_2) \\
 &\quad - \frac{1}{3b} \sin \phi (p_1 - p_2 + p_3 - p_4 + p_5 - p_6) \\
 &= -\sin^2 \phi \left(\frac{dy_R'}{f_R} - \frac{dy_L'}{f_L} \right)
 \end{aligned}$$

The formulae show that only the differences $(dx_R' - dx_L')$, $(dy_R' - dy_L')$, $(df_R - df_L)$ act as error source. Therefore, systematic errors of interior orientation due to camera calibration have no influence for vertical photographs, since the same camera is used for all photos. Convergent photographs, however, use different cameras, and different films with different film shrinkage characteristics, which may cause severe strip bending in bridging but which may be compensated approximately by absolute orientation of the individual model.

From the above formulae weight coefficients are calculable, to study the effect of random errors of interior orientation. These weight coefficients are the elements of the inverse of the normal equation matrix. The normal equation matrix is formed by aid of the parallax equations at the chosen number of orientation points; for Hallert these are six. For example:

$$Q_{\phi\phi'} = \frac{2 \sin^4 \phi \cdot m_{dx'}^2}{f^2 \cdot m_0^2} + \frac{2 \sin^2 \phi \cos^2 \phi \cdot m_f^2}{f^2 \cdot m_0^2}$$

TABLE 2

THE EFFECTS OF INTERIOR ORIENTATION ERRORS ON THE ACCURACY OF RELATIVE ORIENTATION

Column No.	1	2	3	4	5	6
	Convergent		Convergent		Vertical	
m_o	$\pm 6 \mu$	$\pm 6 \mu$	$\pm 20 \mu$	$\pm 20 \mu$	$\pm 20 \mu$	$\pm 20 \mu$
$m_{dx'}, m_{dy'}$	$\pm 20 \mu$	0	$\pm 100 \mu$	0	$\pm 100 \mu$	0
m_f	$\pm 20 \mu$	0	$\pm 50 \mu$	0	$\pm 20 \mu$	0
m_ϕ	$\pm 0.49^c$	$\pm 0.45^c$	$\pm 1.60^c$	$\pm 1.50^c$	$\pm 1.12^c$	$\pm 1.12^c$
m_k	$\pm 0.28^c$	$\pm 0.21^c$	$\pm 1.19^c$	$\pm 0.69^c$	$\pm 0.49^c$	$\pm 0.49^c$
m_ω	$\pm 0.71^c$	$\pm 0.70^c$	$\pm 2.36^c$	$\pm 2.35^c$	$\pm 1.07^c$	$\pm 1.07^c$
m_{bz}	$\pm 0.055 \text{ mm}$	$\pm 0.013 \text{ mm}$	$\pm 0.152 \text{ mm}$	$\pm 0.044 \text{ mm}$	$\pm 0.070 \text{ mm}$	$\pm 0.026 \text{ mm}$
m_{by}	$\pm 0.077 \text{ mm}$	$\pm 0.053 \text{ mm}$	$\pm 0.332 \text{ mm}$	$\pm 0.175 \text{ mm}$	$\pm 0.334 \text{ mm}$	$\pm 0.075 \text{ mm}$

in which $f_R = f_L$, $m_{fR} = m_{fL}$, etc. analogously. These are to be combined with the weight coefficients as determined by Hallert, $Q_{\phi\phi} = h^2/b^2d^2$, to obtain accuracies of exterior orientation elements after orientation, for example:

$$m_{\phi}^2 = m_o^2(Q_{\phi\phi} + Q_{\phi\phi}') = m_o^2 \left(\frac{h^2}{b^2d^2} + \frac{2 \sin^4 \phi}{f^2} \cdot \frac{m_{dx'}^2}{m_o^2} + \frac{2 \sin^2 \phi \cos^2 \phi}{f^2} \frac{m_f^2}{m_o^2} \right)$$

Analogously one obtains:

$$m_{\omega}^2 = m_o^2(Q_{\omega\omega} + Q_{\omega\omega}') = m_o \left[\frac{3h^2}{4d^2} \cos^2 \phi + \frac{2}{3b^2} \sin^2 \phi + \frac{2 \sin^4 \phi}{f^2} \frac{m_{dy'}^2}{m_o^2} \right]$$

$$m_{\kappa}^2 = m_o^2(Q_{\kappa\kappa} + Q_{\kappa\kappa}') = m_o \left[\frac{3h^2}{4d^2} \sin^2 \phi + \frac{2}{3b^2} \cos^2 \phi + \frac{2 \sin^2 \phi \cos^2 \phi}{f^2} \frac{m_{dy'}^2}{m_o^2} \right]$$

$$m_{bz}^2 = m_o^2(Q_{bz bz} + Q_{bz bz}') = m_o \left[\frac{h^2}{2d^2} + \frac{\sin^2 \phi}{f^2} (b^2 \sin^2 \phi + 2bh \sin \phi \cos \phi + 2h^2 \cos^2 \phi) \right. \\ \left. + \frac{m_{dx'}^2}{m_o^2} + \frac{\cos^2 \phi}{f^2} (b^2 \sin^2 \phi - 2bh \sin \phi \cos \phi + 2h^2 \cos^2 \phi) \frac{m_f^2}{m_o^2} \right]$$

$$m_{by}^2 = m_o^2(Q_{by by} + Q_{by by}') = m_o \left[\frac{3h^4}{4d^4} + \frac{h^2}{d^2} + \frac{2}{3} + \frac{2h^2 \cos^2 \phi}{f^2} \frac{m_{dy'}^2}{m_o^2} \right]$$

Table 2 shows a numerical example of the standard errors of the orientation elements for normal-angle convergent photography and wide-angle vertical photography under different assumptions of interior orientation accuracy; m_ϕ , m_κ , m_ω , m_{bz} and m_{by} are computed:

- (1) for the case of careful elimination of interior orientation errors (columns 1 and 2)
- (2) for the case of ordinary plotting procedures, without exercising special care (columns 3 to 6).

The calculations are made for convergent photography (columns 1 to 4) as well as for vertical photography (columns 5 and 6). Note that m_f is larger for convergent photography as compared to vertical photography since two cameras and films are used.

Columns 1, 3 and 5 give orientation errors including error sources of interior orientation. These are not considered in columns 2, 4 and 6, as obtained directly by Hallert's coefficients. The differences between columns 1 and 2, 3 and 4, 5 and 6 represent the influence of interior orientation errors on relative orientation.

The comparison shows that the influence of interior orientation errors on relative orientation remains negligible as long as these remain very small; if they reach amounts of 100μ , as it may happen easily if the diapositives are inserted into the plate carriers by eye, relative orientation is disturbed mainly in κ , by , and bz .

It is therefore essential that:

- (a) an accurate camera calibration of the convergent cameras will ensure the position of the principal-point and the camera constant to $\pm 20\mu$ or better.
- (b) that the diapositives are carefully placed into the plate holders of a carefully calibrated stereoplotter by means of magnifying glasses.
- (c) that a film shrinkage correction according to known and measured fiducial mark distances $f = (a' - a)f/a$ is made from photograph to photograph.

INTERIOR ORIENTATION ERRORS AND AERIAL TRIANGULATION

Further considerations have to be made, if bridging procedures should be applied to convergent photography.

When using the zero base model to join forward and rear pictures of the camera couple of one exposure station, the orientation formulae become:

$$\begin{aligned}
 dbz_L &= \frac{h}{2d} (py_3 - py_5); \\
 hd\phi_L + dbx_i &= \frac{1}{3} (px_1 + px_3 + px_5); \\
 dby_L &= \frac{h^2}{2d^2} (py_3 - py_1 + py_5 - py_1) - py_1; \\
 d\kappa_L &= (px_3 - px_5) \frac{\cos \phi}{2d} - (py_3 - py_1 + py_5 - py_1) \frac{h \sin \phi}{2d^2}; \\
 d\omega_L &= - (px_3 - px_5) \frac{\sin \phi}{2d} - (py_3 - py_1 + py_5 - py_1) \frac{h \cos \phi}{2d^2};
 \end{aligned}$$

by analogous compensation of x and y parallaxes at points 1 to 5 by interior orientation errors we obtain:

$$\begin{aligned}
 dbz_L &= h \cos^2 \phi \left(\frac{df_L}{f_L} - \frac{df_R}{f_R} \right) - h \sin \phi \cos \phi \left(\frac{dx_L'}{f_L} - \frac{dx_R'}{f_R} \right); \\
 hd\phi_L + dbx_i &= h \cos^2 \phi \left(\frac{dx_L'}{f_L} - \frac{dx_R'}{f_R} \right) + h \sin \phi \cos \phi \left(\frac{df_L}{f_L} - \frac{df_R}{f_R} \right); \\
 dby_L &= h \cos \phi \left(\frac{dy_R'}{f_R} - \frac{dy_L'}{f_L} \right) \\
 d\kappa_L &= d\omega_L = 0
 \end{aligned}$$

It becomes evident that:

- (a) the theoretical condition to keep $by_L = by_R$, $bz_L = bz_R$, $bx = b_{\text{cameramount}}$ (Ackermann 1956) should not be maintained in the plotter; it is important to remove all x and y parallaxes in the zero base model, and this, on account of interior orientation errors, will only be possible by using by , bz , and bx , and therefore we obtain the general statement: $by_L \neq by_R$, $bz_L \neq bz_R$ and $bx \neq b_{\text{cameramount}}$.
- (b) bx and ϕ cannot be determined independently. It is common procedure to set $bx = 0$ (or $b_{\text{cameramount}}$) and to move ϕ until the x parallaxes become zero. This

is incorrect since bx should correspond to the unknown interior orientation error. It is therefore best to determine the angle of convergence γ out of the mean between several preliminary zero base model orientations and to keep the difference in ϕ consistently equal to γ for each zero base orientation while bridging. A systematic error in γ will not harm the triangulation result.

- (c) such a procedure will also hold, if errors of synchronization between the two cameras are present. This would still tolerate errors of up to 1/75 sec. (allowing for up to 0.6°/sec. angular velocity of the aircraft), even though most convergent cameras are usually synchronized to $\pm 1/500$ sec.

OTHER FACTORS LIMITING PHOTOGRAMMETRIC ACCURACY

DISTORTION and interior orientation are inseparable according to the physical definition of the optical-axis as the axis of symmetry. Distortion is usually determined from the point of symmetry. Using compensation devices in plotting, a maximum of $\pm 4\mu$ distortion difference is encountered (Hothmer, 1959, pp. 60-78).

Its components $\Delta x'$ and $\Delta y'$ in the photo act as Δx and Δy in the model:

$$\Delta x = \frac{h \cdot f}{(z \cos \phi - x' \sin \phi)^2} \Delta x'$$

$$\Delta y = \frac{hy \sin \phi}{(f \cos \phi - x' \sin \phi)^2} \Delta x' + \frac{h}{f \cos \phi - x \sin \phi} \Delta y'$$

It can be shown that a radial symmetrical distortion has a more favorable effect on convergent than on vertical models. Since in convergent photography two different cameras with different actual distortions may be in use, this may not hold true, however, and it is of prime importance to use cameras in the convergent mount that have been particularly matched or calibrated together.

FILM ERRORS occur during the exposure and during the processing and aging of the exposed material. It is well established that these constitute a major part of photogrammetric inaccuracies. In this respect, a smaller angular field is more favorable than a wider one, for two reasons:

First, the incoming rays at the time of the exposure will hit the emulsion (which is only flat to $\pm 20\mu$) at a lesser angle ($\Delta r = r \tan \alpha$); second, film errors will be enlarged more for wider angle photography because of the bigger magnification ratio. It is immaterial whether vertical or convergent photography of the same angular field is used.

It should be noted, however, that the film of both cameras should be treated similarly in processing; otherwise different regular film shrinkage, particularly different amounts of differential film shrinkage may result.

INSTRUMENT ERRORS. Plotter accuracy is usually independent on whether vertical or tilted photographs are used. It is of importance however that the plotter is carefully calibrated for its interior orientation when convergent photography should be plotted.

The theoretical increased accuracy of convergent photography over vertical photos will be reached only when the above precautions are taken.

PRACTICAL POINT AND BRIDGING ACCURACY

That this is possible was shown by a practical test:

Simultaneously exposed normal angle convergent photography taken by a Zeiss $2 \times$ RMK 21/18 was compared with wide-angle RMK 15/23 photography assuring the same conditions for weather, illumination, film treatment and control. In one strip of 15 and in two strips of 11 models each 278 control points were available. The photography was taken from 15,000 feet. The evaluation was done on a C8.

TABLE 3
ACCURACY COMPARISON FOR SIMULTANEOUS VERTICAL AND CONVERGENT PHOTOGRAPHY

	m_P	m_H
Wide-Angle Vertical: points:	$\pm 0.15^\circ/\text{oo}h$	$\pm 0.12^\circ/\text{oo}h$
Normal-Angle Convergent: points:	$\pm 0.10^\circ/\text{oo}h$	$\pm 0.06^\circ/\text{oo}h$
Wide-Angle Vertical: bridging 15 models	$\pm 0.26^\circ/\text{oo}h$	$\pm 0.26^\circ/\text{oo}h$
Normal-Angle Convergent: bridging 15 models	$\pm 0.24^\circ/\text{oo}h$	$\pm 0.27^\circ/\text{oo}h$

The results of the test are considerably better than any values published thus far. (See Table 3).

Bridging, which can be considered as one of the most crucial tests for the accuracy of a photogrammetric procedure, was successful both in horizontal and vertical accuracy with higher accuracy than corresponding vertical procedures with up to 15 models.

Figure 3 demonstrates position and vertical accuracy versus the number of models bridged for normal-angle convergent and wide-angle vertical photographs.

This indicates a more unfavorable error propagation for convergent photography, which can be found by theory as well, by adding the influences of model orientation with those of the zero base model:

$$\Delta\phi_n = \sum_1^n d\phi_{i\text{Model}} + \sum_0^n d\phi_{i\text{Zero Base Model}}$$

$$\Delta\xi_n = \left(\cos\phi + \frac{h}{b} \sin\phi \right) \left(\sum_1^n d\omega_{i\text{Model}} + \sum_0^n d\omega_{i\text{Zero Base Model}} \right)$$

$$\Delta\xi'_n = \left(\cos\phi - \frac{h}{b} \sin\phi \right) \left(\sum_1^n d\kappa_{i\text{Model}} + \sum_0^n d\kappa_{i\text{Zero Base Model}} \right)$$

$$\begin{aligned} \Delta bz_n = & -b \sum_1^n (n-i)d\phi_{i\text{Model}} - b \sum_1^n (n-i)d\phi_{i\text{Zero Base Model}} \\ & + \sum_1^n dbz_{i\text{Model}} + \sum_0^n dbz_{i\text{Zero Base Model}} \end{aligned}$$

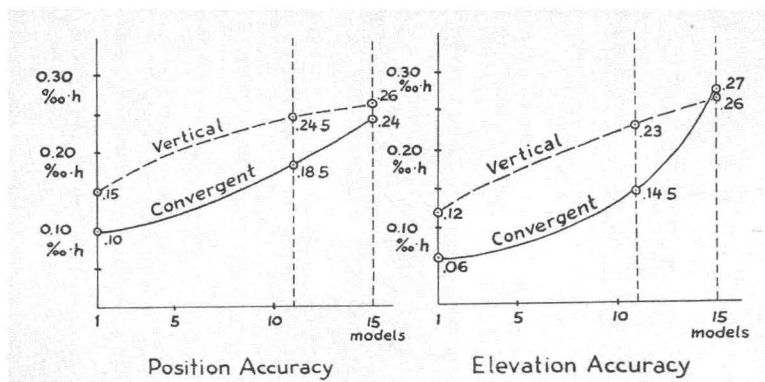


FIG. 3. Bridging Accuracy as a Function of the Number of Models for Vertical and Convergent Photographs.

$$\Delta b y_n = \left(\cos \phi - \frac{h}{b} \sin \phi \right) \cdot b \cdot \left[\sum_1^n (n-i) d\kappa_{i\text{Model}} + \sum_1^n (n-i) d\kappa_{i\text{Zero Base Model}} \right]$$

$$\Delta X_n = -\frac{b}{h} \left\{ \sum_1^n (n-i+1) dz_{i-1} + h \sum_1^n \left[\frac{h}{b} \left(1 + \frac{b^2}{h^2} \right) + \frac{b}{h} (n-1) \right] \cdot (d\phi_{i\text{Model}} + d\phi_{i-1\text{Zero Base Model}}) + \sum_1^n (2n-2i+1) (dbz_{i\text{Model}} + dbz_{i-1\text{Zero Base Model}}) \right\}$$

For 15 models the ratios between the error propagations of normal-angle convergent and wide-angle vertical photography become

for the azimuth 6.1,
 for warping of the strip in flight direction 3.6,
 for warping of the strip perpendicular to flight direction 0.6,
 for scale transfer 5.8.

Considering that for a certain strip length the number of models varies with the type of camera used, this is not nearly as bad as it looks. (See Table 4.)

The test proves that aerial triangulation with convergent photography is feasible, if properly executed.

ANALYTICAL PROCEDURES

Analytical procedures are favorable to the use of convergent photography, particularly if signalized points are used and the photo co-ordinates are measured on a mono-comparator.

It is then that difficulties due to centering of the diapositives, a main source of interior orientation errors, can be avoided, since the fiducial marks can be more precisely read then centered.

Even if calibration errors of a certain camera assembly should be present, these together with eventual distortions can be eliminated analytically, after the camera has taken photographs over a known test area.

An investigation of this nature is currently being made and the results are expected as soon as our new computer installation at U.N.B. becomes operational.

It is up to the individual to decide whether it is of advantage or not to employ the more awkward convergent photography. It is more important, however, to show that theory and practice can be brought into accordance when using proper procedures.

REFERENCES

- Ackermann, F. "Zur rechnerischen Orientierung von Konvergenzaufnahmen." *Bildmessung und Luftbildwissen*, 1956, pp. 24-37.
- Finsterwalder, S. "Eine Grundaufgabe der Photogrammetrie und ihre Anwendung auf Ballonaufnahmen." *Abh. d.K. Bayer. Akad. d. Wissensch. II. Kl., XXII Bd., II. Abt.*, pp. 225-260, 1903.
- Griffin, E. P. "Vertical Photography for Aerotriangulation." *PHOTOGRAMMETRIC ENGINEERING*, 1959.
- Hallert, B. "Some remarks concerning the theory of errors for convergent aerial pictures in comparison with near vertical pictures." *PHOTOGRAMMETRIC ENGINEERING* 1954, pp. 749-757.
- Hothmer, J. "Possibilities and Limitations For Elimination of Distortion in Aerial Photographs." *Photogr. Record*, 1958. II/12 pp. 426-445, 1959. III/13, pp. 60-78.
- Konecny, G. "Aerotriangulation mit Konvergenzaufnahmen." *Veröff d. Deutschen Geodätischen Kommission, Reihe C, Heft 47, Munich* 1962.
- Pennington, J. T. "Aerotriangulation With Convergent Photography." *PHOTOGRAMMETRIC ENGINEERING*, 1954, pp. 76-81.
- Theis, J. B., "Increased Base: Height Ratio." *PHOTOGRAMMETRIC ENGINEERING*, 1958, pp. 127-132.

TABLE 4

NUMBER OF MODELS FOR EQUAL STRIP LENGTH AND DIFFERENT TYPES OF PHOTOGRAPHY

	Based on Equal Photo Scale	Based on Equal Flying Height
Vertical Normal Angle	100	100
Vertical Wide Angle	68	50
Vertical Super Wide Angle	70	29
Convergent Normal Angle	54	52
Convergent Wide Angle	41	24